Molecular Microbiology (2015) 98(4), 743–759 ■
doi:10.1111/mmi.13154
First published online 10 September 2015

PspF-binding domain $PspA_{1-144}$ and the PspA·F complex: New insights into the coiled–coil-dependent regulation of AAA+ proteins

Hendrik Osadnik,[1†] Michael Schöpfel,[2] Eyleen Heidrich,[1] Denise Mehner,[1] Hauke Lilie,[2] Christoph Parthier,[2] H. Jelger Risselada,[3‡] Helmut Grubmüller,[3] Milton T. Stubbs,[2] Thomas Brüser[1*]

[1]*Institute of Microbiology, Leibniz Universität Hannover, Herrenhäuser Str. 2, Hannover 30419, Germany.*
[2]*Institute of Biochemistry and Biotechnology, Martin-Luther University Halle-Wittenberg, Kurt-Mothes-Straße 3, Halle (Saale) 06120, Germany.*
[3]*Max Planck Institute for Biophysical Chemistry, Am Fassberg 11, Göttingen 37077, Germany.*

Summary

Phage shock protein A (PspA) belongs to the highy conserved PspA/IM30 family and is a key component of the stress inducible Psp system in *Escherichia coli*. One of its central roles is the regulatory interaction with the transcriptional activator of this system, the σ^{54} enhancer-binding protein PspF, a member of the AAA+ protein family. The PspA/F regulatory system has been intensively studied and serves as a paradigm for AAA+ enzyme regulation by *trans*-acting factors. However, the molecular mechanism of how exactly PspA controls the activity of PspF and hence σ^{54}-dependent expression of the *psp* genes is still unclear. To approach this question, we identified the minimal PspF-interacting domain of PspA, solved its structure, determined its affinity to PspF and the dissociation kinetics, identified residues that are potentially important for PspF regulation and analyzed effects of their mutation on PspF *in vivo* and *in vitro*. Our data indicate that several characteristics of AAA+ regulation in the PspA·F complex resemble those of the AAA+ unfoldase ClpB, with both proteins being regulated by a structurally highly conserved coiled-coil domain. The convergent evolution of both regulatory domains points to a general mechanism to control AAA+ activity for divergent physiologic tasks via coiled-coil domains.

Accepted 1 August, 2015. *For correspondence. E-mail brueser@ifmb.uni-hannover.de; Tel. +49 511 7625945; Fax +49 511 7625287. †Current address: Department of Microbiology and Immunology, University of California, San Francisco, 600 16th Street, San Francisco, CA 94158, United States of America. ‡Current address: Leibniz Institute of Surface Modification, Permoserstraße 15, Leipzig 04318, Germany.

Introduction

Phage shock protein A (PspA), identified in filamentous phage infected cells of *Escherichia coli* 25 years ago, (Brissette *et al.*, 1990) is the archetype of the conserved PspA/IM30 family that encompasses members in bacteria (Jordan *et al.*, 2006), archaea (Bidle *et al.*, 2008) and plant chloroplasts (Kroll *et al.*, 2001). As part of a stress inducible system (the Psp system, for reviews see Darwin, 2005, Joly *et al.*, 2010, Model *et al.*, 1997, Yamaguchi and Darwin, 2012), PspA was found to interact with two small membrane proteins and putative sensors, PspB and PspC (Adams *et al.*, 2003), as well as with PspF (Dworkin *et al.*, 2000), the transcriptional activator of the system, resulting in a negative feedback-loop. Because of the propensity of PspA to associate with membranes (Brissette *et al.*, 1990) and to oligomerize (Hankamer *et al.*, 2004; Standar *et al.*, 2008), it has been proposed that the Psp system is a membrane stress responsive system. Recent studies strengthen this interpretation, showing that PspA switches interaction partners from PspF to PspBC during overproduction of membrane-weakening, pore-forming secretins (Mehta *et al.*, 2013; Yamaguchi *et al.*, 2013; Flores-Kim and Darwin, 2015). Still, overproduction of several other proteins that do not affect membrane stability also highly induces *psp* (Horstman and Darwin, 2012), suggesting that multiple signals might exist and are integrated in *psp* regulation (Engl *et al.*, 2011). Clearly, a thorough analysis of the regulatory interaction of PspA and PspF, the last, unifying switch in *psp* induction, is imperative for understanding of the system.

PspF is an extensively studied member of the bacterial enhancer-binding proteins (bEBP), specialized AAA+-proteins (Neuwald *et al.*, 1999) needed for alternative sigma factor (σ^{54})-dependent transcription. Briefly, hexameric PspF binds σ^{54} and, via ATP hydrolysis, promotes the open complex formation of the DNA-bound RNA polymer-

ase (Bose *et al*., 2008). The structure of PspF was solved a decade ago (Rappas *et al*., 2005), and numerous studies have probed the function of PspF in transcriptional activation (Chaney *et al*., 2001; Cannon *et al*., 2004; Rappas *et al*., 2005; 2006; Joly *et al*., 2006; Bose *et al*., 2008; Burrows *et al*., 2010; Zhang *et al*., 2013; Sharma *et al*., 2014). The interaction with its regulator PspA (which in *trans* takes the part of the usual *cis*-regulatory domains of other bEBPs) is however poorly understood. It is known that PspA and PspF can form a complex (Joly *et al*., 2009), which leads to inhibition of ATPase activity (Elderkin *et al*., 2002) and down-regulation of *psp* expression *in vivo* (Dworkin *et al*., 2000). It is thought that the PspA·F complex likely consists of 6 PspA per 6 PspF (Elderkin *et al*., 2002; 2005; Joly *et al*., 2009; Zhang *et al*., 2013). An exposed loop on PspF around Trp56 has been identified as a PspA-binding determinant (Elderkin *et al*., 2005; Zhang *et al*., 2013), and the PspF-binding region (FBR) in PspA has been localized in the fragment $PspA_{1–186}$ (Elderkin *et al*., 2005; Joly *et al*., 2009), with a recent study suggesting that residues 25–40 form an amphipathic helix important for PspF inhibition (Jovanovic *et al*., 2014). Still, the lack of any PspA/IM30 family structure precludes a detailed understanding of the proteobacterial PspA·F complex as well as other PspA-like proteins on a molecular level.

In vitro work with full-length or fragmented PspA has been challenging, as the stability of activity strongly relied on the addition of detergents (Elderkin *et al*., 2002). We overcame those issues by identifying the PspF regulatory core domain in PspA that lacks membrane-interacting or oligomerization properties and is fully functional in the absence of detergent over longer periods of time with respect to PspF-binding and inhibition *in vivo* and *in vitro*. We present the crystal structure of this domain at 1.8 Å resolution, identify the PspF-binding surface and characterize regulatory influences of single amino acid exchanges on the activity of PspF *in vivo* and *in vitro*. The PspA·F complex has a striking resemblance to the AAA+ unfoldase ClpB (Lee *et al*., 2003) and its regulatory middle domain, showing that regulation of AAA+ proteins via coiled-coil domains evolved convergently for AAA+ proteins of diverse functions.

Results

Identifcation of $PspA_{1–144}$, the PspF-inhibiting domain of PspA

The σ^{54} activator PspF is an important example for a AAA+ family protein that does not contain intrinsic regulatory domains, but instead is regulated by another protein, PspA, in *trans*. On a molecular and structural level, it is still largely unresolved how this regulation is achieved, and we therefore intended to obtain more information about the involved structures and interactions. PspA is difficult to study as it can not only interact with PspF, but also with membrane components such as PspC or lipids (Brissette *et al*., 1990; Adams *et al*., 2003), and it can self-associate to form large superstructures (Hankamer *et al*., 2004; Standar *et al*., 2008). To circumvent issues arising from those characteristics that are unrelated to the PspA–PspF interaction, we sought to identify the minimal PspF-interacting domain of PspA. A previous fragmentation approach that was based on a helical domain prediction (HD1–4, Fig. 1A; Elderkin *et al*., 2005, Joly *et al*., 2009) already indicated that PspF-binding determinants are located in the not oligomerizing fragment $PspA_{1–186}$. However, $PspA_{1–186}$ was less effective than full-length PspA ($PspA_{1–222}$) in PspF-ATPase inhibition (Joly *et al*., 2009), still partially associated with the membrane and was purified by a protocol that employs detergent to preserve solubility (Elderkin *et al*., 2005; Jovanovic *et al*., 2014), indicating that $PspA_{1–186}$ still contains determinants unrelated to PspF-binding. It is thus important to recognize possible functional domains in PspA. In previous studies, PspA was predicted to comprise a large number of more or less likely coiled-coils that are organized in four helical domains (Joly *et al*., 2009). When we performed a coiled-coil prediction using COILS, the outcome was much less complex. COILS predicted three large coiled-coil regions (CC1–3) that did not correspond to the helical domains that were the basis of earlier fragmentation approaches (Fig. 1A). Importantly, CC2 ended at amino acid 144, which is 42 residues earlier than the end of the previous $PspA_{1–186}$ construct. As it is known that regions within the first 67 residues and after residue 110 are important for PspF regulation (Joly *et al*., 2009), it seemed possible that CC1 and CC2 are responsible for PspF regulation, and that the 42 amino acid extension of CC2 in $PspA_{1–186}$ somehow supports the membrane interaction of this construct (Jovanovic *et al*., 2014).

We thus generated $PspA_{1–144}$, which comprises the native N-terminal region (NTR) and only the two predicted coiled-coil domains CC1 and CC2 (orange, Fig. 1A). $PspA_{1–144}$ and full-length PspA turned out to essentially indistinguishably inhibit PspF-dependent *psp* expression in a Δ*pspA* reporter strain over the course of 15 hours, suggesting that both interact similarly with PspF (Fig. 1B, left). Neither protein had a negative effect on growth (Fig. 1B, right). However, the two proteins differed in their subcellular localization. In agreement with previous analyses, overproduced full-length PspA localized to both the membrane and cytoplasmic fractions (Yamaguchi *et al*., 2010). In contrast, $PspA_{1–144}$ was exclusively soluble, indicating that the membrane-interacting trait of PspA had been removed (Fig. 1C). Consequently, we were now able to purify his-tagged $PspA_{1–144}$ from the cytoplasmic frac-

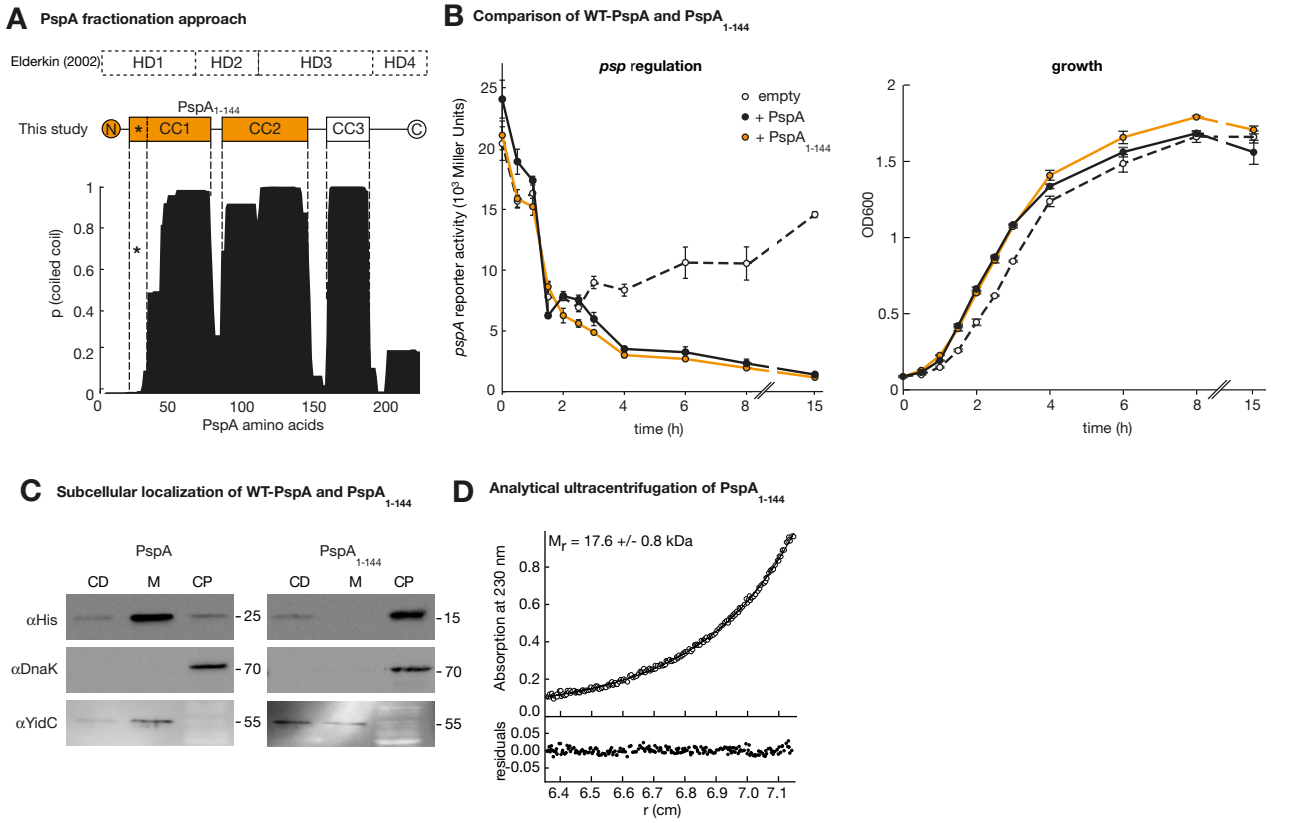

Fig. 1. Identification of the minimal PspF-inhibitory domain of PspA, $PspA_{1–144}$.
A. Bottom: COILS prediction for PspA. Top: Domain structure of PspA as derived from the COILS prediction, $PspA_{1–144}$ (*orange*) highlighted. For comparison, the proposed helical domains HD1-4 of PspA as suggested by Elderkin *et al.* (2005) are indicated earlier.
B. Comparison of full-length PspA and $PspA_{1–144}$ in *psp* regulation. Both have strong and indiscernible inhibitory effects. Left: LacZ-activity assay in a MC3 Δ*pspA* reporter strain showing the inhibitory effect of $PspA_{1–144}$ (*orange*) and full-length PspA (*black*) relative to an empty vector control (*dashed line*) when overproduced. Right: Growth curves for the cultures used for LacZ-activity assays.
C. Western blot with antibodies against the His-tag showing that $PspA_{1–144}$ localizes to the soluble fraction after ultracentrifugation, while full-length PspA is found in both the membrane and cytoplasmic fraction. Signals of the control proteins DnaK (CP) and YidC (M) in the samples are given to show that the fractionation was successful. CD, cell debris; M, membrane; CP, cytoplasmic fraction.
D. Sedimentation equilibrium of $PspA_{1–144}$ during analytic ultracentrifugation indicates that $PspA_{1–144}$ is purely monomeric *in vitro*. The curve fit corresponds to a mass of 17.6 kDa (monomeric $PspA_{1–144}$ ≈ 17.55 kDa).

tion without the need of detergents for keeping the protein in solution. Subsequent equilibrium sedimentation experiments (analytic ultracentrifugation, AUC) showed that purified $PspA_{1–144}$ was exclusively monomeric (Fig. 1D), indicating that it also lacks the determinants for self-association. Thus, PspF interaction is mediated by a domain that comprises the N-terminal 2/3rds of PspA, whereas self-association as well as detectable membrane interaction require the truncated C-terminal regions, possibly including CC3.

Crystal structure of $PspA_{1–144}$ reveals similarity to the M-domain of the AAA+ protein ClpB

Having the stable, monomeric and soluble PspF-interacting PspA domain at our hands, we were able to crystallize this protein and solved its structure to a resolution of 1.8 Å (Fig. 2A). This is the first member of the conserved PspA/IM30 family to be crystallized. $PspA_{1–144}$ forms an extended monomeric structure in which the two coiled-coil regions CC1 and CC2 (see Fig. 1A) form an intramolecular anti-parallel coiled-coil (Pro25-Arg142) linked by a tip region (Ala75-Leu91). A short NTR (Ile3-Val11) covers a hydrophobic patch on CC1 (Fig. 2A, Fig. S1A-C), connected to CC1 by a flexible linker (residues Asn12-Glu23), with Asp24 acting as an *N*-cap to the CC1 helix. Three highly flexible residues in this linker (Lys20, Ala21, Glu23) could not be resolved. In atomistic molecular dynamics simulations that included these residues, the NTR remained attached to the coiled coil while the flexibility of the linker was confirmed (Fig. S1D,E). Conservation of residues contributing to intramolecular coiled-coil stabilization (Fig. 2B, green) and tip formation (red) within proteins of the PspA/IM30 family indicates

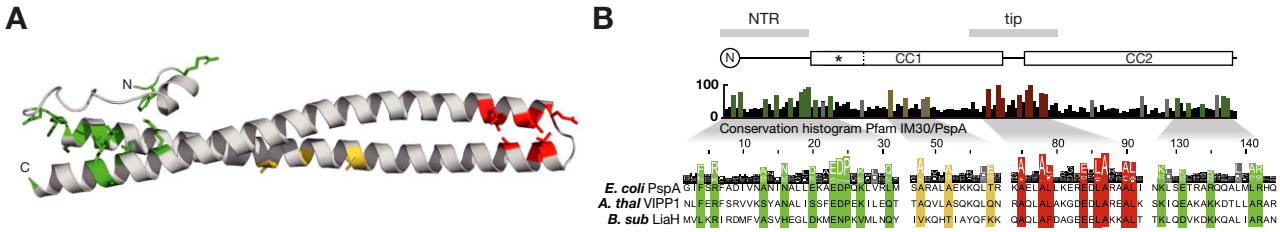

Fig. 2. The crystal structure of PspA$_{1–144}$ shows the conserved architecture of PspA/IM30 family proteins. Conserved amino acids: *green, red*- structurally important amino acids; *yellow*- others.
A. Crystal structure of PspA$_{1–144}$ shown in *cartoon* representation, conserved residues as *sticks*. The short loop of amino acids 23–24 was modelled as no electron density for these residues was observed.
B. Overall conservation histogram and detailed excerpts for well-studied members of the PspA/IM30-family. For orientation, CC-domains of PspA$_{1–144}$ (as in Fig. 1A), N-terminal region (NTR) and tip domain (tip) are indicated earlier.

that the *E. coli* PspA$_{1–144}$ structure presented here reflects the general architecture of this family, including the well-studied VIPP1 from chloroplasts and LiaH from *Bacillus subtilis*.

A search for structurally related proteins using the program DALI (Holm *et al.*, 2008) yielded a number of coiled-coil containing protein domains (as expected for such a common structural element) of varying lengths and little to no functional similarity. Interestingly, PspA$_{1–144}$ showed significant structural similarity (*Z*-score 6.6, top 10% of all hits) to the coiled-coil M-domain of the ClpB family of AAA+ unfoldases/disaggregases, although they have alternative permutations of the secondary structure elements, as CC1 of PspA is represented by two helical domains in ClpB (Fig. 3B and C), which is known to decrease the *Z*-score of similar folds (Holm and Rosenstrom, 2010). This domain (ClpB-MD), which is found as an insertion within the AAA+ domain and adorns the peripheral surface of the hexameric ring, regulates the disaggregase activity of ClpB by modulating its ATPase activity (Schirmer *et al.*, 2004; Oguchi *et al.*, 2012). The highly similarly sized PspA$_{1–144}$ and ClpB-MD superimpose with an r.m.s.d. (root-mean-square deviation) of 1.1 Å for backbone atoms (Fig. 3A; see Fig. S2 for stereo images).

Variants of PspA$_{1–144}$ reveal a FBR on CC1

We investigated residues of PspA$_{1–144}$ that are responsible for PspF binding and regulation by characterizing the phenotypes of amino acid substitutions in CC1 positions that are conserved in γ-proteobacteria (Fig. S3A), suggestive of a possible interaction interface with the likewise conserved PspF. When produced in a P$_{pspA}$-lacZ reporter strain with a Δ*pspA* background, several of these PspA$_{1–144}$ variants resulted in less *psp* repression in comparison to the wild-type fragment (including R30A and E37A,

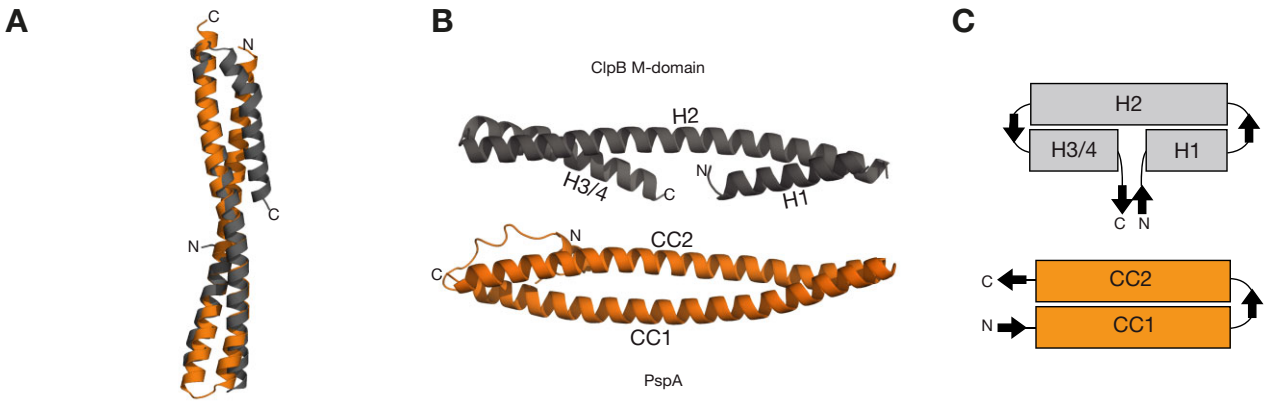

Fig. 3. PspA$_{1–144}$ (*orange*) is structurally highly similar to the M-domain of ClpB (ClpB-MD).
A. Superimposition of the backbones of coiled-coiled moieties of both proteins using Swiss-PdbViewer (Guex and Peitsch, 1997). For stereo representations see Fig. S3.
B. Side by side comparison of PspA and ClpB-MD structure as *cartoon* representation, schematically depicted in (C). CC1 of PspA is divided into two helices (H3/4 and H1) in ClpB-MD, but secondary structure and backbone directions are conserved (*arrows* indicating N- to C-terminal direction).

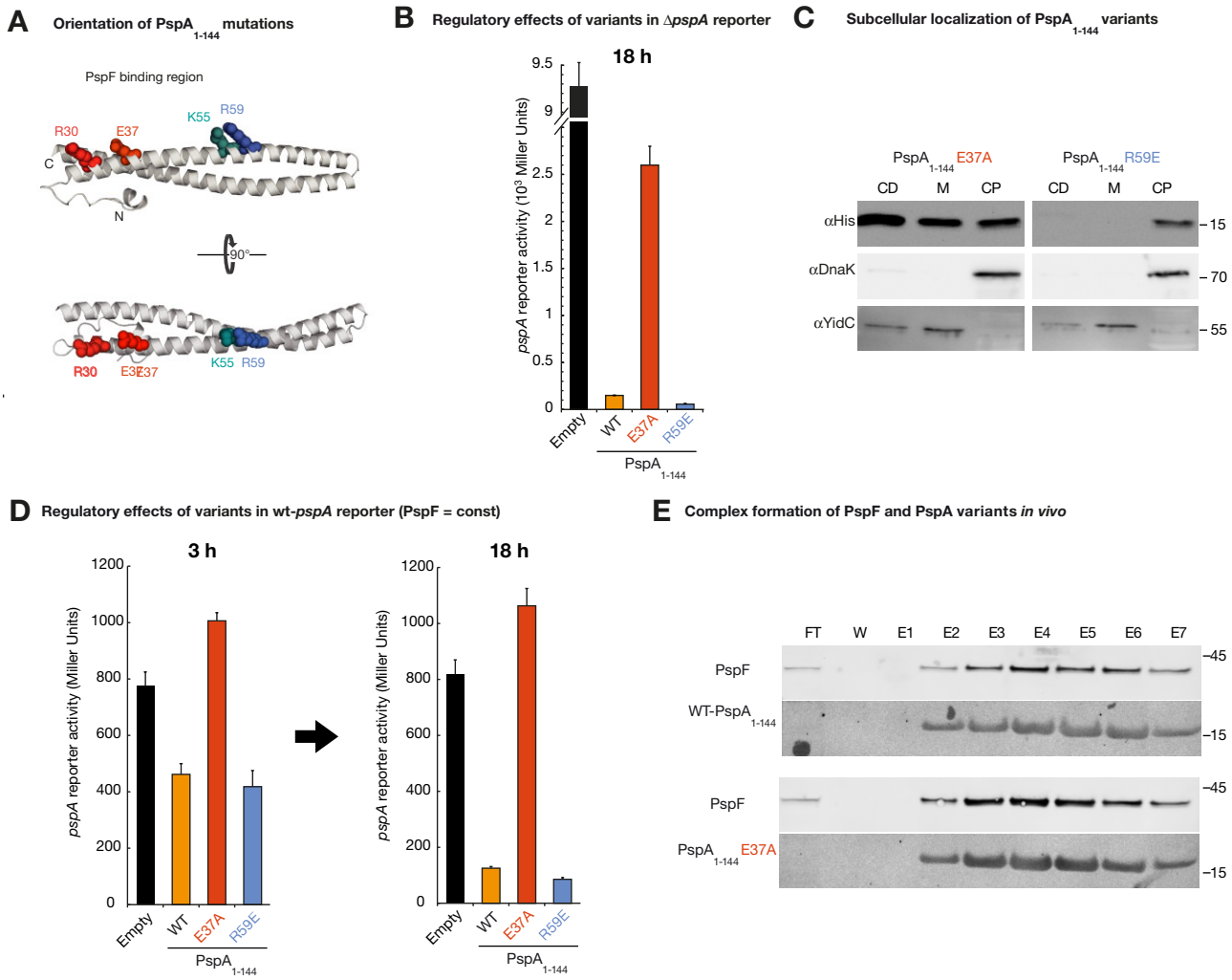

Fig. 4. Effects of single amino acid exchanges E37A (*red*) and R59E (*blue*) in the putative PspF-interacting region of PspA.
A. Variants that change PspF inhibition *in vivo* cluster on one side of PspA (cf. Fig. S3).
B. LacZ-activity assays (MC3 *ΔpspA*) showing changes in PspF-inhibitory effect of $PspA_{1–144}$ variants relative to WT-$PspA_{1–144}$ (*orange*) and compared to the unregulated empty vector control (empty). $PspA_{1–144}$-E37A is a weaker, $PspA_{1–144}$-R59E is a stronger inhibitor of *psp*. Long-term induction was needed to dilute the high LacZ concentration of the unregulated *ΔpspA* reporter strain.
C. Subcellular localization of both $PspA_{1–144}$ variants. Both fragments are present in the cytoplasm, but $PspA_{1–144}$-E37A is also found in inclusion bodies and the membrane fraction. For localization of the wild-type fragment and used abbreviations see Fig. 1C.
D. LacZ-activity assays in a wild-type *pspA* background with constant expression of *pspF* (MC3 *ΔpspF pUL-pspF-strep*) showing that $PspA_{1–144}$-E37A induces *psp* above the level of the empty vector control (empty). $PspA_{1–144}$-R59E leads to slightly stronger repression than the wild-type. Effects are already detectable after 3 h of induction (left), and get more pronounced after long-term induction (right).
E. Co-elution of strep-tagged PspF with his-tagged $PspA_{1–144}$-E37A from the reporter strain after 3 h shows that both proteins interact *in vivo* while the variant induces *psp*. Wild-type $PspA_{1–144}$ is shown as comparison. Western blots of Ni-IMAC using equal amounts of the flow-through (FT), last wash fraction (W) and the seven elution fractions (E1–E7), using antibodies against the Strep- and His-tag, respectively.

Fig. S3B). Additionally, amino acid substitutions at the very C-terminal end of this conserved region caused more effective repression than the wild-type (R59E, Fig. S3C). Two results of this preliminary screen were especially noteworthy: First, all single amino acid exchange variants retained PspF inhibition to a certain degree since all measured *psp* levels were markedly below the level of the uninhibited control indicating that these single amino acid exchanges did not fully abolish the functional interaction. Second, the surface-exposed exchanges with pronounced effects on *psp* regulation clustered on one side of PspA, which suggested to us that we might have identified the FBR on PspA (Fig. 4A and Fig. S3D).

To address this important aspect further, we extensively characterized two $PspA_{1–144}$ derivatives in more detail: $PspA_{1–144}$-E37A, the strongest loss-of-repression variant of a surface residue, exhibiting a ~20-fold loss in repression; and $PspA_{1–144}$-R59E, the only derivative causing

enhanced repression relative to the wild-type fragment (0.3-fold *psp* level, Fig. 4B). Both variants were present in the cytoplasm at a concentration roughly similar to the wild-type fragment (Fig. 4C, compared with Fig. 1C, all localizations were done in parallel). If anything, the amount of $PspA_{1–144}$-R59E seemed to be slightly lower, indicating that the enhanced repression due to this mutation is not an effect of higher protein concentration. We found $PspA_{1–144}$-E37A to also form inclusion bodies that resulted in a pronounced accumulation in the cell debris and membrane fractions. As will be shown later, the protein in the soluble fraction nevertheless is monomeric and functional.

We undertook a detailed *in vivo* analysis of the effects of the two regulatory variants on PspF using a wild-type *pspA* reporter strain. Our previous experiments were performed in a Δ*pspA* reporter strain with a strong uninhibited *psp* promoter activity (up to 25 000 Miller Units shortly after inoculation from an overnight culture, Fig. 1B). This made prolonged induction times necessary to dilute previously accumulated LacZ, not leaving the option to examine differential effects of variants on PspF directly after induction. We therefore tested effects of our variants in the wild-type *pspA* genetic background, which has a balanced *psp* expression that is maintained by the autoregulatory feedback-loop of PspA-dependent PspF inhibition. To ensure that our repression-phenotypes were not caused by varying PspF levels in our reporter strains, endogenous *pspF* was deleted, and *strep*-tagged PspF was maintained at a constant level by expressing its gene constitutively from a low-copy plasmid. Western blots confirmed that PspF levels were indeed comparable between the strains at all times (Fig. S4A).

As expected in this pre-regulated Psp system, changes in *psp* levels because of the expression of $PspA_{1–144}$ variants in the PspA wild-type background were already visible after 3 h (Fig. 4D, left) and became more pronounced after 18h (Fig. 4D, right). $PspA_{1–144}$-R59E caused a slight increase in PspF repression relative to WT-$PspA_{1–144}$ at 3 h with significantly enhanced repression after 18 h, consistent with the data obtained in the Δ*pspA* strain (Fig. 4B). $PspA_{1–144}$-E37A induced *psp* above wild-type level at both time points, turning from a less-effective inhibitor in the Δ*pspA* background to an activator in the wild-type *pspA* background. We performed co-elution experiments of the soluble fraction to investigate whether this activating effect was still due to direct interaction with PspF, or whether it was a secondary effect because of the partial inclusion body formation of that variant. Both $PspA_{1–144}$ and $PspA_{1–144}$-E37A co-elute PspF-*strep* with indiscernible strength, indicating that $PspA_{1–144}$-E37A directly interacts with PspF in the cytoplasm of *E. coli* while simultaneously inducing the Psp system (Fig. 4E). These co-elution experiments were performed using the same induction time and strength at which we observed the activating effect. These results are in full agreement with the regulatory data obtained with the Δ*pspA* strain, where $PspA_{1–144}$-E37A significantly inhibited the PspF-dependent promoter activity, which can most easily be explained by an interaction of $PspA_{1–144}$-E37A with PspF *in vivo* (Fig. 4B). We ensured that this effect was not due to the elevated PspF levels by showing that the effect of $PspA_{1–144}$-E37A was even stronger in the wild-type *psp* background, i.e. a strain without deletion and *trans*-complementation of the *pspF* locus (Fig. S4B). The activating effect of the E37A mutation in a wild-type *psp* background was unexpected, as the intrinsic repression by endogenous PspA should override expression of a loss-of-function variant as $PspA_{1–144}$-E37A. It is therefore highly remarkable that a variant of $PspA_{1–144}$ is dominant over the wild-type PspF inhibition mechanism without being able to regulate PspF at least as effectively as intrinsic PspA. We also found evidence that the activating effect of the E37A mutation was not confined to the $PspA_{1–144}$ fragment, but that it also existed in the context of full-length PspA: In a wild-type *psp* background, the E37A mutation led to a 6.7-fold induced *psp* level relative to the empty vector control (Fig. S4C). It has to be mentioned that this up-regulation, although strong and significant, cannot fully be attributed to the E37A mutation alone, as un-mutated full-length PspA already slightly induced *psp* after long-term production (2.8-fold), which was a largely PspBC-dependent effect in this experimental setup and thus not a direct effect of the PspA–PspF interaction *per se* (Fig. S4D). We could further confirm that the E37A variant of full-length PspA still bound PspF comparable with the wild-type full-length protein (Fig. S4E). While the E37A mutation therefore seems to have a comparable physiologic effect in the full-length and truncated fragment, this experiment once more shows the advantage of working with $PspA_{1–144}$, as it is not prone to secondary effects on PspA·F interaction that can result from oligomerization with the pool of intrinsic PspA as well as from membrane and/or PspBC interaction.

Six PspA monomers bind one hexamer of PspF

We further characterized the PspA–PspF interaction *in vitro*. Size exclusion chromatography experiments using purified $PspA_{1–144}$ and $PspF_{1–265}$ (a stably folding variant lacking the C-terminal DNA-binding domain) clearly showed complex formation of $PspA_{1–144}$ and $PspF_{1–265}$ (Fig. S5A). Using AUC, we investigated the dynamics of $PspA_{1–144}$·$PspF_{1–265}$ complex formation (for simplicity, called PspA·F complex from now on) in detail. Titrating $PspA_{1–144}$ to $PspF_{1–265}$ demonstrated a micromolar dissociation constant ($K_D \approx 1$ μM, Fig. 5A). The most strongly *psp*-inducing FBR-variant $PspA_{1–144}$-E37A bound $PspF_{1–265}$ with slightly reduced affinity ($K_D \approx 6$ μM), whereas the

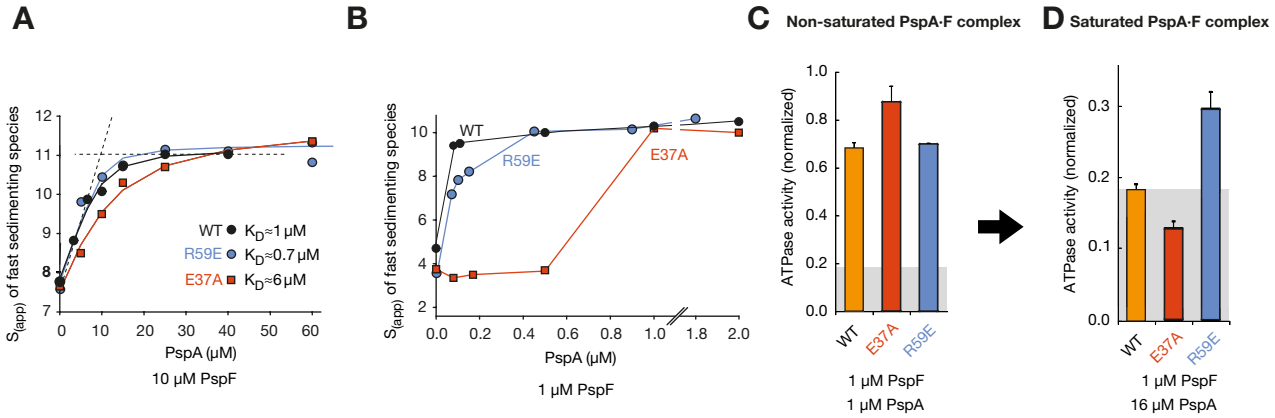

Fig. 5. PspA and PspF form a highly stable complex with a basal ATPase activity *in vitro*. (A/B) In analytic ultracentrifugation experiments (AUC), $PspA_{1–144}$, $PspA_{1–144}$-E37A or $PspA_{1–144}$-R59E were titrated in variable concentrations to $PspF_{1–265}$ and the change of the sedimentation coefficient (Svedberg) of the fast-sedimenting PspA·F species as a function of PspA concentration was determined.
A. Addition of PspA to 10 μM $PspF_{1–265}$, a concentration at which PspF readily self-oligomerizes. The K_D was determined for both WT and variants, determination of complex stoichiometry (1 to 1 binding of WT-PspA) is shown as dashed lines that cross at around 10 μM PspA.
B. Stabilizing effect of PspA and its variants at low concentrations of PspF. At 1 μM $PspF_{1–265}$, where PspF is mostly non-hexameric, addition of very low amounts of $PspA_{1–144}$ already lead to formation of a fast-sedimenting PspA·F species. Variants show either slightly less ($PspA_{1–144}$-R59E) or nearly no ($PspA_{1–144}$-E37A) stabilization at sub-stoichiometric concentrations.
C. $PspF_{1–265}$ exhibits K_D-dependent inhibition of its ATPase activity by PspA variants under non-saturating conditions.
D. Variants change the basal ATPase activity (grey) of the PspAF complex. This effect does not correspond to their differences in K_D.

super-inhibitory variant $PspA_{1–144}$-R59E showed binding comparable to the WT ($K_D \approx 0.7$ μM). Furthermore, the stoichiometry of binding could be shown to be 1:1 in all cases. As PspF is mostly hexameric at these concentrations (10 μM, Fig. S5B), this ratio corresponds to a complex of six $PspA_{1–144}$ with six $PspF_{1–265}$, which is in full agreement with earlier studies (Joly *et al.*, 2009; Lenn *et al.*, 2011; Mehta *et al.*, 2013; Jovanovic *et al.*, 2014). As $PspA_{1–144}$ is a monomer, these results suggest that one hexamer of PspF possesses six distinct binding sites for monomeric PspA, analogous to the hexameric AAA+ core of ClpB that can interact with the six coiled-coil regulator domains independently.

One PspA monomer is sufficient to stabilize one hexamer of PspF

While examining PspF hexamerization using AUC, we observed that $PspF_{1–265}$ does not oligomerize spontaneously when present in low concentration (1μM, Fig. S5B), which is relevant as PspF is thought to exist in low concentration, i.e. just ~130 copies per cell (Jovanovic *et al.*, 1997, PspA: ca. 1500 copies, Valgepea *et al.*, 2013). We therefore wondered whether PspA would also interact with monomeric PspF, or whether PspF needed to hexamerize first. Published gel filtration data using PspF variants suggest that a PspA·F complex is formed independently of the starting oligomeric state of PspF, yet in these experiments both proteins were pre-incubated at high concentrations and PspA was added in excess (Joly *et al.*, 2009).

To our surprise, addition of very low concentrations of PspA (0.08 μM) to 1μM PspF resulted in the emergence of one fast-sedimenting species of PspA·F (9.4 S, Fig. 5B). At these concentrations, PspA only contributed less than 2 % of the overall UV absorption in the sample cell. The fast-sedimenting species therefore comprised around 0.46 μM PspF in the sample cell (~ 46% of total UV absorption, Fig. S5C). Taking the ratio of applied PspA to shifted PspF into account (0.08:0.46 μM or 1:5.8), these data show that one monomer of $PspA_{1–144}$ is able to bind and stabilize one hexamer of $PspF_{1–265}$ over the course of the AUC measurement. No intermediary complexes could be observed. In contrast, $PspA_{1–144}$-E37A was found to stabilize PspF hexamers only above equimolar concentrations (Fig. 5B, Fig. S5C), while $PspA_{1–144}$-R59E showed slightly impaired ability to form complexes at low concentrations. These results indicate that sub-stoichiometric PspA stabilizes PspF hexamers and also supports the idea that we have identified a PspA interface important for binding. We would like to note that, while certainly interesting for PspA–PspF interaction studies, PspA-dependent stabilization cannot be a basic prerequisite for PspF hexamerization *in vivo*, as PspF is active in a Δ*pspA* strain (Fig. 1B). Therefore, most likely the C-terminal DNA-binding region of PspF, which had to be truncated for effective purification in our experiments, stabilizes PspF hexamers *in vivo*, as suggested before (Schumacher *et al.*, 2004). The PspA-mediated sub-stoichiometric stabilization of PspF hexamers may thus play only a very minor physiological role, possibly by contributing to the

long-term stability of active PspF. Typically, AAA+ proteins are also strongly bound and stabilized by nucleotides. PspF is unusual in this respect as it binds ATP or ADP only weakly. (Joly *et al.*, 2006) Although PspF hexamers are stabilized by nucleotides at protein concentrations above 9 μM (Joly *et al.*, 2006), AUC measurements with near-physiologic 1 μM $PspF_{1–265}$ indicated no stabilizing effect, even at ADP concentrations of 0.5 mM (ca. fivefold K_D, Fig. S6D, cf. Joly *et al.*, 2006).

Fully saturated PspA·F complex has a basal ATPase activity that can be increased or decreased by PspA variants

The central function of the PspA·F complex, regulation of PspF-dependent transcriptional activation, is tightly linked to the ATPase activity of PspF (Elderkin *et al.*, 2005). Therefore, we examined the influence of WT-$PspA_{1–144}$ and its FBR-variants $PspA_{1–144}$-E37A and $PspA_{1–144}$-R59E on the ATPase activity of PspF *in vitro*. As predicted, $PspA_{1–144}$ strongly reduced PspF-ATPase activity (Fig. 5C). However, even the saturated PspA·F complex showed a significant residual ATPase activity of ~18% (Fig. 5D), in accordance with the previous finding that inhibition of PspF-ATPase remains incomplete in the presence of either fragments or full-length PspA (Elderkin *et al.*, 2002; 2005; Joly *et al.*, 2009). As this basal ATPase activity might have been due to an association–dissociation equilibrium of the complex (leading to brief periods of uninhibited PspF following PspA dissociation), we measured the increase of PspF activity after jump dilution, which is dependent on PspA dissociation (Fig. S7A). From these data we determined the half-life for PspA·F to be 43 min ($k_{off} = 2.69 \cdot 10^{-4}\ s^{-1}$), which strongly argues against fast exchange rates of PspA protomers of PspA·F complexes. In ATPase assays with PspA in sub-saturating concentrations, we found that the strength of ATPase inhibition was dependent on the K_D of the PspA–PspF interaction (Fig. 5C). $PspA_{1–144}$ and $PspA_{1–144}$-R59E with virtually the same K_D inhibited PspF stronger than $PspA_{1–144}$-E37A, which has a sixfold higher K_D). However, in assays with PspA-saturated complexes, this K_D-dependence disappeared: In the presence of saturating PspA, the residual ATPase activity of PspF was 30% lower with $PspA_{1–144}$-E37A and 30% higher with $PspA_{1–144}$-R59E as compared to WT-$PspA_{1–144}$ (Fig. 5C). Thus, wild-type or mutated variants can have distinct effects on PspF ATPase that do not necessarily correlate with effects on transcriptional activity of PspF: The exchange E37A leads to a lower ATPase activity *in vitro*, but higher *psp* induction *in vivo*, and *vice versa* for R59E. As we will discuss in detail later, this disconnection of ATPase and transcriptional activity is counterintuitive, but in agreement with previously reported effects of mutations in the PspF-σ^{54} system.

Atomistic simulations indicate a possible PspA·F complex structure

We tested PspA·F complex formation and stability in a series of atomistic molecular dynamics simulations based on the assumption that six PspA monomers should contact PspF with their FBR and that one of the interaction sites on PspF should be at the W56-loop (Elderkin *et al.*, 2002; Zhang *et al.*, 2013). In one upright orientation in which the binding region contacted both the W56-loop of one PspF protomer and an ATP binding helix (sensor-II domain) on the adjacent PspF, PspA remained bound to PspF during the time course of the simulation (138 ns, four independent simulations) (Fig. S6A, complex depicted in Fig. S6B). In control simulations (in which the binding epitopes on PspA pointed away from PspF), PspA failed to maintain a stable interaction (Fig. S6A). While these simulations are by no means exhaustive, they demonstrate the possibility that PspA engages two PspF protomers, which might explain the stabilization of PspF hexamers by sub-stoichiometric PspA.

Discussion

In this study, we examined the regulatory mechanism of PspA·F-dependent *psp* induction *in vivo* and *in vitro*. We identified the PspF regulating domain of PspA, $PspA_{1–144}$, a large coiled-coil formed by the helices CC1 and CC2 (Fig. 1A). This large fragment, comprising two-thirds of PspA, was as effective as the full-length protein in *psp* regulation (Fig. 1B). In previous studies, shorter fragments showed impaired PspF interaction (Elderkin *et al.*, 2005; Joly *et al.*, 2009), which clearly indicates that this domain is necessary and sufficient for PspF regulation under non-stress conditions. Because of its monomeric and stably soluble nature (Fig. 1C and D), $PspA_{1–144}$ allowed us to look at characteristics of the PspA·F complex that eluded observation so far, and it furthermore led us to the first crystal structure of the PspA/IM30 protein family. The conservation of residues that are important for this structure indicates that the PspA architecture must be highly conserved throughout the PspA/IM30 family (Fig. 2B).

Full-length PspA is partially membrane localized and oligomeric whereas $PspA_{1–144}$ is soluble and monomeric. This is fully compatible with evidence in the literature that point toward a cooperative role of the N- and C-terminal parts of PspA in oligomerization and functions at the membrane. Previous studies have indicated that either deletion of an N-terminal helix (Jovanovic *et al.*, 2014) or point mutations in a part or the C-terminus (Yamaguchi *et al.*, 2010) lead to a change in membrane/PspBC interaction. Given this evidence that membrane-dependent functions rely on having both N- and C-termini present, it

is not surprising that we find an exclusively cytoplasmic location for $PspA_{1–144}$, lacking its C-terminus. Importantly, the short N-terminal amphipathic helix (residues 2–19) that has previously been implied to interact with membranes (Jovanovic *et al.*, 2014), is laterally docked against CC1 and CC2 in our structure (Fig. S1D). Our structure may thus represent a membrane-detached state with the NTR back-folded to the coiled-coil in some kind of 'parking' position, ready to be released for membrane interactions upon some signal. However, this helix alone is clearly not sufficient to mediate a stable membrane interaction of monomeric $PspA_{1–144}$. The PspF-regulatory domain (CC1 and CC2, residues 23 to 144) is likely not involved in membrane binding, since there is no evidence from the crystal structure for a direct membrane interaction: No amphipathic patches (with exception of those in the folded coiled-coils) are present in this part of the protein, and there are no discernible regions of positively charged surface amino acids, either of which would presumably be important for a direct membrane interaction.

The monomeric state of $PspA_{1–144}$ likely results from lack of CC3 and the far C-terminal region. This view is in full agreement with previous analyses that suggested a key role of C-terminal regions in PspA for oligomerization and effector function, as a $PspA_{1–186}$ fragment was already strongly affected in both respects (Joly *et al.*, 2009; Jovanovic *et al.*, 2014). We note that CC3 contains a consensus-motif for short parallel trimeric coiled-coils (amino acids 174–179, see Kammerer *et al.*, 2005), which might indicate that PspA forms trimers when initializing oligomerization. It is however uncertain at this point how exactly oligomerization is achieved and whether or not parts of $PspA_{1–144}$ have to interact with C-terminal regions directly. The lack of membrane interaction and oligomerization made $PspA_{1–144}$ suitable for crystallization and PspA·F complex studies. It must be kept in mind that the $PspA_{1–144}$ construct and the analyzed derivatives thereof are useful to selectively address the regulatory PspF interaction without interfering aspects of membrane interaction, such as recruitment of PspA by PspBC or the effector function. However, we would like to stress that the PspA–PspF interaction certainly has to be seen in the context of the full-length protein and the Psp system it is part of to fully understand the physiologic role of proteins of the PspA/IM30 family. Furthermore, the now established coiled-coil structure of $PspA_{1–144}$ has to be kept in mind when interpreting effects of PspA fragments that have helices partially removed from within the coiled-coil, which certainly can result in non-physiologic secondary effects because of structural destabilization of the protein and exposition of amphipathic helices that lack their coiled-coil counterpart.

Using $PspA_{1–144}$ for mechanistic studies, we were able to characterize the PspA·F complex as a highly stable complex with a 6:6 stoichiometry and a basal ATPase activity *in vitro*. If the stability of the $PspA_{1–144}$·$PspF_{1–265}$ complex *in vitro* (half-life ~ 43 min, Fig. S5E) resembles that *in vivo*, then the high stability of the complex constrains the mechanism of regulation of *psp in vivo* and an entirely dissociation-based mechanism that relies on indirect activation of *psp* via sequestering free PspA to the membrane does not suffice for a rapid *psp* response. It may thus be required that PspA has to be more actively 'peeled off' PspF during induction either by conformational changes in PspA (e.g. mediated by the C-terminus) and/or by conformational changes upon interactions with PspBC or the membrane (Yamaguchi *et al.*, 2013).

Our results support the possibility that PspF activity can in principle be altered without a requirement for PspA·F complex dissociation. An *in vivo* screen for PspF-inhibition variants of $PspA_{1–144}$ allowed us to identify a surface patch on PspA that is likely responsible for the regulatory PspF interaction, stretching along the length of the coiled-coil on the side of the protein opposite to the back-folding N-terminus. Detailed characterization of two PspF-regulation variants of $PspA_{1–144}$ show that mutations in this region can alter the activity of PspA-regulated PspF, likely while bound to PspF (a modulatory interaction), leading to a change in *psp* levels *in vivo* as well as in the basal ATPase activity of PspF *in vitro*: The up-regulating effect of $PspA_{1–144}$-E37A is a dominant phenotype in a wild-type background while this fragment clearly binds PspF (Fig. 3D and E). Therefore, the bound $PspA_{1–144}$-E37A represses PspF less effectively than the wild-type protein, which may mimic a post-binding level of PspF regulation in the case of our PspA fragment. Similar post-binding effects on the ATPase activity can be observed *in vitro*, where the basal activity of the saturated PspA·F complex seems to be modulated by variants relative to the wild-type (Fig. 4D). Interestingly, the mutation E37A, which led to an induction of *psp in vivo* relative to the wild-type fragment (Fig. 3B, also visible in the full-length PspA, Fig. S4C), exhibited a lower ATPase level in the saturated complex *in vitro*, and the R59E mutation that led to a higher basal ATPase level *in vitro* repressed *psp* stronger than wild-type $PspA_{1–144}$ *in vivo* (Fig. 5C).

With the current model of PspF-dependent *psp* regulation in mind, these observations are counterintuitive. However, our results are not unprecedented, as mutations in either PspF or σ^{54} have similar effects. Although wild-type PspA–PspF-σ^{54} exhibits a linear correlation between ATPase activity and transcriptional activation, the mutated system does not: Zhang *et al.* (2013) produced PspF variants essentially without ATPase activity yet hyperactive transcriptionally (e.g., variant G58C). Additionally, enhancer-bypass mutations of σ^{54} can fully alleviate the requirement for a bEBP (Syed and Gralla, 1997; Chaney and Buck, 1999). Hence, the energy dependence of tran-

scriptional activation in the natural EBP-σ^{54} system is likely used for tight transcriptional control (see e.g.Sharma *et al*., 2014). Thus, even though it was unexpected that PspA seems to change the coupling of ATPase and transcriptional activity in PspF while bound to it, the observed effects are similar to those of described variants of PspF and σ^{54}. How could the effect of PspA variants be explained mechanistically? With the emerging pattern for AAA+ function being that controlled, sequential ATPase activity of subunits is highly important (see e.g., Carroni *et al*., 2014, Glynn *et al*., 2009, Sysoeva *et al*., 2013). The PspA variant R59E might lead to a slight desynchronization of PspF subunits, resulting in a higher raw ATPase activity, but decrease in physiologic efficacy of the bEBP, while variant E37A acts vice versa. A modulatory role of PspA would be in agreement with previous reports, which indicated that PspA can interact with PspF in all its conformational states during transcriptional activation: a PspA·F complex still binds to σ^{54}, and PspA interacts stably with ADP-AlF_x trapped PspF·σ^{54} complexes (Joly *et al*., 2009) that are thought to mimic the transcription activating state of PspF (Chaney *et al*., 2001; Burrows *et al*., 2010).

PspA-dependent modulation of PspF could be employed in two ways: Either to ensure a controlled low-level *psp* production under non-stress, or to serve as a second mode of stress-dependent induction. The activity of *psp* in the exponential growth phase (~1500 copies of PspA;Li *et al*., 2014, Valgepea *et al*., 2013) has been so far attributed to the presence of slight membrane stresses (Jovanovic *et al*., 2014), but our data allow another interpretation: The basal ATPase level of the saturated PspA·F complex indicates that PspA-dependent PspF activity might be kept at a controlled basal level by bound PspA. Our R59E variant indeed indicates that *psp* could be more repressed *in vivo* than it actually is by bound wild-type PspA, and the long half-life might prevent the complex from sensing varying PspA levels via PspA dissociation under non-stress conditions. A tightly controlled basal induction of *psp* might therefore be advantageous for the cell to keep the Psp system in check, and could explain why the PspA-dependent regulation of PspF does not interfere with PspF oligomerization or σ^{54} interaction (Joly *et al*., 2009). Alternatively, modulation of PspF could also add a second layer of *psp* induction that may be achieved by slight conformational changes upon stress signals, which would enable a rapid and fine-tuned stress response. While strong induction of *psp* undoubtedly relies on the dissociation of PspA, as clearly observed for secretin stress (Yamaguchi *et al*., 2013), it will be interesting to see how the PspA–PspF interaction changes under other stresses where *psp* is comparably slightly induced, e.g. salt stress (Weber *et al*., 2006), and if a modulatory action of bound PspA could play a role there. Hence, although we found strong evidences suggesting a modulatory regulation of PspF by PspA, it is unclear at this point how relevant these effects are under different conditions *in vivo*. Most importantly, with the current level of molecular understanding, we do not know whether the variants of PspA that we produced mimic actual states in the cycle of PspF regulation or not. We also cannot exclude that, although unlikely in our opinion, the tendency of $PspA_{1–144}$-E37A to form inclusion bodies might have indirect effects on the Psp system. We see however a strong interaction of the variant with PspF in the cytoplasm of *E. coli* as well as clear binding, a modulation of PspF-ATPase activity and no sign of aggregation or inactivity *in vitro*, suggesting that the inclusion body formation does not interfere with assessment of PspF inhibition in our experimental setup.

While being an insulated occurrence in bEPB regulation, we found that PspA·F system shares several structural and mechanistic features with ClpB. It is interesting to note that the typical regulation of bEBPs happens at the level of hexamerization: Regulatory domains act exclusively on the assembly state of the AAA+ ATPase, allowing formation of an active oligomeric bEBP only in the presence of an inducing signal (Doucleff *et al*., 2005; De Carlo *et al*., 2006). PspF, however, is active per default (Jovanovic *et al*., 1996), and regulated by PspA in a post-assembly mechanism (Elderkin *et al*., 2002). While PspA·F therefore differs from canonical bEBP regulation, our studies reveal that a structurally similar regulator can be found in members of the ClpB family of AAA+ proteins, where the middle domain (ClpB-MD), a coiled-coil resembling PspA (Fig. 3), regulates the activity of the protein. From a strictly physiologic perspective, ClpB and PspA·F have completely different roles: One is a disaggregase, responsible for unfolding of misfolded proteins under stress conditions (Woo *et al*., 1992), the other is involved in the regulation of gene expression (Jovanovic *et al*., 1996). Also, ClpB's middle domain is fused to the AAA+ domain, while in PspA·F, PspA acts in *trans*. Their common feature is the hexameric AAA+ core that provides the driving force behind both protein functions. We found several similarities: PspA·F and ClpB have the same stoichiometry (6:6), and both show a basal ATPase activity (Seyffer *et al*., 2012, this study). Our simulations of the PspA·F complex also hints toward a possible interaction of PspA with two protomers of PspF (Fig. S6), which is a feature of ClpB, where the middle domain likely interacts with two neighboring subunits (Oguchi *et al*., 2012). Additionally, helix 3 of ClpB-MD and its counterpart on PspA, the N-terminal part of CC1, contain residues crucial for the regulation of the AAA+-domain (e.g. Y503A in ClpB,Oguchi *et al*., 2012; E37A in PspA, this study), indicating at least partial structural overlap of regions of AAA+ interaction. Nevertheless, this does not mean that both system are regulated in exactly the same way, as ATPase activity in both systems

is harnessed for two different tasks: ClpB pulls aggregated peptides apart using repeated ATPase cycles (Lum *et al.*, 2004), while PspF, as discussed earlier, adds an energy barrier to a process that does not need energy *per se*, allowing for highly specific induction. As a consequence, we note that the effects of amino acid variants on ATP hydrolysis are different and seem to be stronger in ClpB than in PspA·F (PspA E37A; ATPase activity 30 % down, *psp* levels ~20-fold up), but translate into comparably weaker effects on physiologic activity (e.g. ClpB K476C; ATPase ~15-fold up, disaggregase activity ~3-fold up, Oguchi *et al.*, 2012). Future studies will shed more light on the molecular mechanism of PspF regulation, and the crystal structure of the PspA·F complex, followed by a thorough mutational study of the PspA–PspF interface, is certainly needed to reach the level of understanding that exists for middle domain-dependent ClpB regulation (see Haslberger *et al.*, 2007, Mogk *et al.*, 2003, Oguchi *et al.*, 2012, Schirmer *et al.*, 2004).

At last, it remains to be seen whether this general regulatory mechanism is used by other, less well-characterized AAA+ proteins as well, and how the mechanism has adapted to its respective task. Although different in certain aspects, the similarities of ClpB and PspA·F show that a coiled-coil domain, either covalently fused to the AAA+ domain or non-covalently bound, can act as a regulator of diverse AAA+ proteins. A tempting, but speculative question that remains is, why a member of the conserved PspA/IM30 family 'hijacked' a bEBP for its own regulation in the proteobacterial system: Did the conserved PspA/IM30 family coincidentally happen to have a structure that made bEBP-dependent regulation of its own production in proteobacteria possible, even though the structure evolved for a physiologically different reason, such as membrane stabilization? Or did the PspA/IM30 family *per se* (co-)evolve as regulators of the ubiquitous AAA+ domain, which in turn allowed PspA in proteobacteria to regulate its own production?

While we hope to have laid the foundations for a more detailed understanding of the PspA/IM30 protein family in general, and the intricate regulatory features of the proteobacterial PspA·F complex in particular, many features concerning the action of PspA/IM30 remain obscure. Twenty-five years after its first description, there is still much to discover in the field of PspA.

Experimental procedures

Strains and cultivation

For all protein purifications, *E. coli* strain BW25113 (Datsenko and Wanner, 2000) with indicated plasmids was used. The strain MC3 (Bergler *et al.*, 1994), a derivative of *E. coli* MC4100 (Casadaban, 1976) harboring a *pspA* promoter fused to *lacZ* integrated into the λattachment site, was used to investigate changes in WT *psp* level via LacZ-activity assays. Prior to first use, the arabinose-resistance of this strain was assured via plating on LB containing 1 % (w/v) arabinose. The same clone was used for all further transformations and transductions to ensure that observed differences in *psp* induction were not a result of different intracellular arabinose levels in the tested strains (Lindenstrauss *et al.*, 2010). Its derivative MC3 *ΔpspA::kan* was constructed via P1-phage transduction (Thomason *et al.*, 2007) of MC3 using the *ΔpspA::kan* containing JW1297 from the Keio collection (Baba *et al.*, 2006). MC3 *ΔpspF::kan* was obtained similarly, using JW1296. All cultures were grown while shaking at 37°C in LB medium (1% (w/v) tryptone, 1% (w/v) NaCl, 0.5% (w/v) yeast extract) if not otherwise specified and supplemented with ampicillin (100 μg ml^{-1}) where appropriate.

Genetic methods and plasmids

The fragment of *pspA* coding for $PspA_{1–144}$ was cloned using the respective primers (Table S1) and chromosomal DNA as template. The primers contained restriction sites (5′-NcoI; 3′-XhoI) for cloning into the *pBAD-pspA-H_6* plasmid previously constructed (Standar *et al.*, 2008), leading to a short leucine-glutamate linker in front of the C-terminal hexahistidine tag. Site-directed mutagenesis based on the QuikChange protocol (Agilent, Waldbronn, Germany) was performed to exchange bases in *pBAD-pspA-H_6*. Primer pairs and the resulting change on amino acid level are given in Table S1 ('*pspA-ex-*'). To allow easier molecular access to the region coding for the PspF-binding patch, a BspHI restriction site was introduced by a silent mutagenesis at base pairs 92–98 of *pspA* (coding for amino acids Leu31 to Ile33) resulting in *pBAD-pspA-H_6-BspHI*. This plasmid was then used for several base exchanges that were coded in a primer overhang and cloned into the plasmid using either NcoI/BspHI or BspHI/XhoI respectively (Tab. S1, '*pspA-BspHI-*'). For cloning of *$pspF_{1–265}$* into *pBW22* (Wilms *et al.*, 2001), *$pspF_{1–265}$* was amplified using chromosomal DNA as template. Primers contained restriction sites (5′-NdeI; 3′-BamHI). For construction of the pSC101-based constitutive low-copy expression system pUL-P_{tat}, the P_{lac}-promoter-containing NdeI/XbaI fragment of pCHAP418 (Possot *et al.*, 1992) has been removed by excision, Klenow treatment and religation, and a 436 bp fragment containing the constitutive *E. coli tatA* promoter with an engineered NdeI site at the tatA start codon has been amplified using pABS-*tatABC* (Berthelmann and Brüser, 2004) as template, and ligated into the PstI/HindIII sites of the vector. The coding region of *E. coli pspF* was then cloned into pUL-P_{tat} (Tab. S1) using NdeI/HindIII. All plasmid constructs were verified by DNA sequencing.

Biochemical methods

Standard protein purification. Overnight cultures were diluted to an OD of 0.05. After induction with 0.1 % (w/v) arabinose (or rhamnose in case of pBW-*$pspF_{1–265}$-H_6*) and further growth for 3 h, cells were centrifuged at 6000 × *g* (4°C) and pellets stored at −18°C. Cells were suspended in 20 mM Tris/HCl, 100 mM NaCl and 20 mM imidazole (pH 8.0) and disrupted by two French Press passages at 138 MPa

and 4°C. Afterwards, cell debris was removed using low-speed centrifugation at 6000 × *g* (20 min, 4°C), and membranes and soluble fractions were further separated using ultracentrifugation (Beckman Optima L-80 XP, Beckman Coulter, Krefeld, Germany, 140 000 × *g*, 1 h, 4°C). Protein was taken exclusively from the soluble fraction and purified via Ni-NTA agarose resin (Qiagen, Hilden, Germany) using standard Ni-affinity protocols. Samples were further purified by anion exchange (Resource Q, GE Healthcare, Freiburg, Germany, linear gradient from 0 to 1 M NaCl in 20 mM Tris/HCl pH 8.0) resulting in pure protein as controlled via Coomassie Brilliant Blue stained SDS-PAGE gels and SEC. For long-term storage, the ionic strength was readjusted to 100 mM NaCl with HiTrap desalting columns (GE Healthcare, Freiburg, Germany) and protein was concentrated by ultrafiltration (Vivaspin 10 000 MWCO, Sartorius Stedim, Goettingen, Germany). Because of the high stability of $PspA_{1–144}$ and $PspF_{1–265}$, proteins could be stored at –80°C in 20 mM Tris/HCl and 100 mM NaCl without additives and behaved like freshly prepared samples in all assays (ATPase activity, AUC, SEC) after thawing. All protein concentrations were calculated via their extinction coefficient and absorption at 280 nm. To assess and compare the subcellular localization of PspA, $PspA_{1–144}$, and its variants, the pellet of low-speed (cell debris) and ultracentrifugation were resuspended in a buffer volume equal to the supernatant, and aliquots were analyzed via SDS-PAGE/Western blotting, using polyclonal anti-PspA antibodies (Standar *et al*., 2008), anti-DnaK, anti-YidC or monoclonal anti-His-tag antibodies (Qiagen, diluted 1:5000) and the corresponding secondary antibodies coupled to horse radish peroxidase for enhanced chemoluminescence (ECL) detection. All steps of the localization experiments shown in Fig. 1C and Fig. 4C were performed simultaneously. For co-elution experiments, Ni-affinity purifications from the cytoplasmic fraction of cell cultures were performed as described earlier. After Western blotting, his-tagged PspA (or its fragments and variants) and strep-tagged PspF were detected in the samples using monoclonal anti-StrepTag II (EMD Millipore, Billerica, USA) and His-probe (Santa Cruz Biotechnology, Dallas, USA) antibodies and detected using the respective goat secondary antibodies (IrDye 800CW and 680LT) and the Odyssey system (Li-Cor, Lincoln, USA).

Purification of selenomethionine labeled $PspA_{1–144}$ *(Se-PspA).* Se-PspA-producing cells were grown in minimal medium M9 (Sambrook and Russell, 2001) with 0.4 % (w/v) glucose as carbon source and 0.1 % (v/v) SL12 trace element solution (Overmann *et al*., 1992). Incorporation of selenomethionine (Acros Organics, now Thermo Fisher Scientific, Geel, Belgium) was assisted by suppression of methionine biosynthesis (Van Duyne *et al*., 1993) 15 min prior to induction. Purification of Se-PspA was performed similar to that of unlabeled protein, except that 5 mM 2-mercaptoethanol was added throughout all purification steps and in the storage buffer to keep Se-PspA in a reduced state.

Crystallization, data collection and structure determination of $PspA_{1–144}$*.* Purified $PspA_{1–144}$ in 10 mM Tris/HCl buffer (pH 8.0) and 50 mM NaCl at a final concentration of up to 9 mg ml^{-1} was used for crystallization by the vapor diffusion hanging drop method. 1 µl $PspA_{1–144}$ was mixed with an equal volume of crystallization buffer containing 0.1 M HEPES/NaOH (pH 7.5), 10 % (w/v) polyethyleneglycol 6000 and 5 % (v/v) 2–methyl–2,4–pentanediol and incubated at 15°C. Final high resolution diffracting crystals where obtained by macro-seeding of initial $PspA_{1–144}$ crystals at a protein concentration of 2 mg ml^{-1} using a refined crystallization buffer containing 0.1 M HEPES/NaOH (pH 7.2), 10% (w/v) polyethyleneglycol 6000 and 5% (v/v) 2–methyl–2,4–pentanediol. Se-$PspA_{1–144}$ in 10 mM Tris/HCl buffer (pH 7.5), 50 mM NaCl and 5 mM 2-mercaptoethanol was crystallized in the same manner, but using native $PspA_{1–144}$ crystals for cross-seeding. Crystals of both native and Se-containing $PspA_{1–144}$ appeared after 3 days and reached their final size within 1 week. Prior to flash-freezing, the crystals were cryo-protected by addition of 15% (v/v) (R,R)-(-)-2,3-butanediol (Merck Millipore, Darmstadt, Germany) to the mother liquid. Collection of the native and the three MAD datasets was carried out under cryogenic conditions (100 K) at the BESSY synchrotron beamline 14.1 (Helmholtz Zentrum, Berlin, Germany) and processed with the XDS package (Kabsch, 2010) (see Table S2 for statistics). Phase determination was carried out by multiple wavelength anomalous dispersion (MAD) using the Se-$PspA_{1–144}$ datasets. The heavy atom substructure (four selenium sites) was determined and refined using SHELX (Sheldrick, 2010) and SHARP followed by density modification using SOLOMON within the autoSHARP pipeline (Vonrhein *et al*., 2007). The resulting electron density map was of sufficient quality to allow automated tracing and model building using the programs ARP/wARP (Langer *et al*., 2008) and BUCCANEER from the CCP4 suite (Winn *et al*., 2011). The generated model was subjected to further cycles of manual building and refinement employing the programs COOT (Emsley *et al*., 2010) and Refmac5 (Murshudov *et al*., 1997) using the highest resolution (1.8 Å) native dataset and Translation/Libration/Screw (TLS) refinement for final refinement cycles. The final structure model of PspA covers residues Ile3 to Glu20 and Asp24 to Arg142, remaining residues were not visible in the electron density. Residues Asn12 to Leu31 show significantly higher conformational diversity than the rest of the structure as reflected by higher B-factors and poorly defined electron density in this region. It is assumed that the less ordered regions in the PspA structure are also the origin of the structural refinement converging at slightly higher R-factors (see Table S2). The structure was validated using Molprobity (Chen *et al*., 2010) and deposited at the Protein Data Bank (PDB) under the accession ID 4WHE.

LacZ-activity assays. Activity of *psp* reporters in different strains was assessed using the classic activity assay by Miller (Miller, 1972). Generally, all overnight cultures were diluted to an OD of 0.05 and allowed to grow for 3 more hours (induced with 0.1 % arabinose) before LacZ-activity was assessed. Where indicated ('18 h'), prolonged induction was used to discriminate between *psp* inhibiting and *psp*-inducing fragments of PspA. Only in those assays, media for overnight cultures already contained 0.1 % (w/v) arabinose to induce production of *psp* regulating fragments from pBAD vectors. All measurement were done in triplicate (error bars in figures correspond to one standard deviation). Where indicated, intrinsic controls [at least a *pBAD22* empty vector control (Guzman *et al*., 1995) and a $PspA_{1–144}$ producing strain] were used for normalization to ensure comparability.

ATPase assays. Measurements were performed in assay buffer containing 20 mM Tris/HCl, 100 mM NaCl and 10 mM $MgCl_2$ at pH 8.0 in triplicate. As PspA stabilizes PspF hexamers and the PspA–PspF interaction was found to be extremely stable, care was taken to ensure that $PspF_{1–265}$ was equilibrated at nearly the final concentration for 1 h prior to addition of PspA at the indicated final concentrations from concentrated stock solutions. Following another 15 min of preincubation at 30°C, the assay was started by the addition of 2 mM ATP (final concentration) and samples were taken at the indicated time points. The amount of accumulated phosphate released during ATP hydrolysis was subsequently measured using a colorimetric assay (Lanzetta *et al.*, 1979), modified as described (Turgay *et al.*, 1997). In all cases, negative controls without PspF were carried along to subtract (the generally very low) background effects. For jump dilution experiments, $PspA_{1–144}$ (30 μM) and $PspF_{1–265}$ (20 μM) were preincubated for 60 min and the assay was started by diluting the sample 1:40 into assay buffer already containing 2 mM ATP. Samples were taken at the indicated time points. Samples containing 0.5 μM PspF and 0.75 μM PspA were prepared as described earlier and equilibrated for 60 min before starting the measurement. Their ATP hydrolysis rate (triplicate) was determined to be 0.1387 μM s^{-1} and served as reference. The k_{off} was subsequently estimated numerically with the nls algorithm of *R*[8](200 000 iterations) using the reference hydrolysis rate and the data obtained for the jump diluted sample (Copeland *et al.*, 2011). With dissociation being a first-order reaction, the half-life of the complex could then be calculated as $t_{1/2} = \frac{0.693}{k_{off}}$ (Tummino and Copeland, 2008).

Size exclusion chromatography. SEC (ÄKTA Explorer, GE Healthcare) was used to investigate complex formation of $PspA_{1–144}$ and $PspF_{1–265}$. Proteins ($PspF_{1–265}$ at 130 μM, $PspA_{1–144}$ at 210 μM) were preincubated at indicated molar ratios for 10 min at 4°C, 1 μM of ATP (Carl Roth, Karlsruhe, Germany) or AMPPNP (Sigma-Aldrich, Taufkirchen, Germany) and 10 mM $MgCl_2$ were added where indicated. A 100 μL aliquot of the sample was then applied to a Superose 6 10/300 GL column (GE Healthcare) equilibrated with 20 mM Tris/HCl and 100 mM NaCl adjusted to pH 8.0 at a flow rate of 0.5 ml min^{-1} and 4°C. Elution profiles were obtained measuring the absorption of the effluent at 230 nm.

AUC. All measurements were performed in 20 mM Tris, pH 8, 100 mM NaCl at 20°C using an Optima XL-A centrifuge (Beckman, Palo Alto, CA, USA), an An50Ti rotor, and double-sector cells. Depending on protein concentration and addition of cofactors, e.g. ADP, the distribution of the protein in the cell was monitored at 230, 260, 280 or 300 nm. Data were analyzed using the software SedFit (Schuck, 2000). Isolated $PspA_{1–144}$ was investigated at concentrations of 3, 10 and 30 μM. Sedimentation velocity measurements were made at 40 000 r.p.m. for 4 h, sedimentation equilibrium was performed at 14 000 r.p.m. Sedimentation of PspF was measured at concentrations of 1–30 μM at 40 000 r.p.m. (velocity run) and 14 000 or 5000 r.p.m. (sedimentation equilibrium). Complex formation of PspF with $PspA_{1–144}$ was determined at initial concentrations of PspF of 1, 10 and 30 μM, respectively by titration of $PspA_{1–144}$ to maximal 60 μM. Sedimentation velocity of the complex was measured at 40 000 r.p.m., sedimentation equilibrium at 5000 r.p.m.

In silico *methods*

Coiled-coil prediction. Coiled-coil predictions for PspA (Uniprot accession: P0AFM6) were performed using the COILS algorithm (Lupas *et al.*, 1991) with a prediction frame of 21 amino acids for most accurate identification of coiled-coil ends (according to the COILS/PCOILS manual, see also Gruber *et al.*, 2006) and MTIDK matrix. The window size of 21 amino acids also increases the prediction accuracy relative to smaller window sizes, yet it can be assumed to be sufficiently small to not decrease the resolution of the prediction (Gruber *et al.*, 2006). Results were similar whether weighting was enabled or disabled and did not change significantly using an aligned input sequence (PCOILS algorithm).

Consensus sequences. Sequences of γ-proteobacterial members of PspA/IM30 were obtained from the Pfam database (Punta *et al.*, 2012). Clearly too short sequences lacking larger parts of the primary sequence were discarded, yielding 715 sequences. Redundancies were reduced to prevent overrepresentations and the consensus logo histogram was calculated using Jalview (Waterhouse *et al.*, 2009). The overall PspA/IM30 consensus was similarly prepared using the Pfam RP35 representative proteome sequences of the PspA/IM30 family (165 sequences from all phyla). In all consensus histograms, a score of 0 indicates no conservation at this position, 100 indicates full conservation in all proteins.

Structure comparison and modelling. A DALI (Holm *et al.*, 2008) search was performed with the PspA structure (PDB-ID 4WHE). For subsequent detailed comparison of ClpB and PspA coiled-coil structures, backbones of the coiled-coil forming protein moieties ($ClpB_{399–513}$, PDB-ID 4HSE; $PspA_{27–141}$, PDB-ID 4WHE) were superimposed in the Swiss-PdbViewer (Guex and Peitsch, 1997) using 'magic fit' and 'explore fragment alternative fit' algorithms, as primary sequence alignment failed because of the difference in domain order in PspA and ClpB (see Fig. 3C). The highest scoring fit had an r.m.s.d. of 1.10 Å for 284 overlapping backbone atoms with an overall score of 68. This fit was used for all subsequent comparisons and simulations. Missing loops of PspF (PDB-ID 2BJW) and PspA (PDB-ID 4WHE) were modelled with COOT (Emsley *et al.*, 2010). For oligomeric complex prediction of PspA·F, the hexameric oligomer of PspF was constructed using GalaxyGemini (Lee *et al.*, 2013) with subsequent energy minimization. ClpB was then fitted into the PspF hexamer with Pymol (Schrodinger, 2010) using only the AAA+-domain of ClpB (PDB-ID 4HSE) for superimposition. PspA was then fitted into the M-domain of the previously aligned ClpB to obtain a model for the fully saturated PspA·F complex.

Simulations. The atomistic molecular simulations of PspA·F complexes were performed with Gromacs (Hess *et al.*, 2008) (version 4.6) using the AMBER99SB-ILDN force field

(Lindorff-Larsen *et al*., 2010) with the TIP4P water model. Virtual sites were used to allow the usage of a larger integration time step (0.003 fs). The Particle Mesh Ewald method was used to calculate electrostatic interactions. A simulation box was fitted around the protein complex consisting of 6 PspA and 6 PspF, which allowed 2 nm distance from the periodic boundaries. The temperature in the simulations was coupled to an external heat bath of 303 K using the velocity rescale method (tau_t = 0.1 ps). The external pressure was coupled to 1 bar using the Berendsen barostat (compressibility = 4.5×10^{-5} bar^{-1}, tau_p = 1.0 ps). Four independent simulations were performed for PspA·F complexes either based on ClpB-like M-domain orientation (18 ns of simulated time) or with various upright orientations of PspA at the PspF hexamer surface for a simulated time of 129–145 ns (138 ns on average).

Acknowledgements

We would like to thank Sybille Traupe and Inge Reupke for preparation of strains and plasmids used in this study, Michael Ringel for help with programming and Uwe Müller (Freie Universität Berlin at BESSY) for synchrotron time. We would furthermore like to thank Kürşad Turgay, Noël Molière and Carol Gross for discussions and critical reading of the manuscript. This work was supported by the German Research Foundation (DFG grant BR2285/4-1).

Author contributions

HO and TB designed the experiments, MS did the crystallization and MS, CP, and MTS solved the structure of PspA, EH and DM contributed localization data and part of the activity data, HL did AUC analyses, HJR and HG contributed MD simulations, HO performed all other experiments, HO, HL, MTS, and TB evaluated the data and HO, MTS, and TB wrote the article.

Conflict of interest

The authors declare that they have no conflict of interest.

References

Adams, H., Teertstra, W., Demmers, J., Boesten, R., and Tommassen, J. (2003) Interactions between phage-shock proteins in *Escherichia coli*. *J Bacteriol* **185:** 1174–1180.

Baba, T., Ara, T., Hasegawa, M., Takai, Y., Okumura, Y., Baba, M., *et al*. (2006) Construction of *Escherichia coli* K-12 in-frame, single-gene knockout mutants: the Keio collection. *Mol Syst Biol* **2:** 2006 0008.

Bergler, H., Abraham, D., Aschauer, H., and Turnowsky, F. (1994) Inhibition of lipid biosynthesis induces the expression of the *pspA* gene. *Microbiology* **140** (Part 8): 1937–1944.

Berthelmann, F., and Brüser, T. (2004) Localization of the Tat translocon components in *Escherichia coli*. *FEBS Lett* **569:** 82–88.

Bidle, K.A., Kirkland, P.A., Nannen, J.L., and Maupin-Furlow, J.A. (2008) Proteomic analysis of *Haloferax volcanii* reveals salinity-mediated regulation of the stress response protein PspA. *Microbiology* **154:** 1436–1443.

Bose, D., Pape, T., Burrows, P.C., Rappas, M., Wigneshweraraj, S.R., Buck, M., and Zhang, X. (2008) Organization of an activator-bound RNA polymerase holoenzyme. *Mol Cell* **32:** 337–346.

Brissette, J.L., Russel, M., Weiner, L., and Model, P. (1990) Phage shock protein, a stress protein of *Escherichia coli*. *Proc Natl Acad Sci USA* **87:** 862–866.

Burrows, P.C., Joly, N., and Buck, M. (2010) A prehydrolysis state of an AAA+ ATPase supports transcription activation of an enhancer-dependent RNA polymerase. *Proc Natl Acad Sci USA* **107:** 9376–9381.

Cannon, W.V., Schumacher, J., and Buck, M. (2004) Nucleotide-dependent interactions between a fork junction-RNA polymerase complex and an AAA+ transcriptional activator protein. *Nucleic Acids Res* **32:** 4596–4608.

Carroni, M., Kummer, E., Oguchi, Y., Wendler, P., Clare, D.K., Sinning, I., *et al*. (2014) Head-to-tail interactions of the coiled-coil domains regulate ClpB activity and cooperation with Hsp70 in protein disaggregation. *Elife* **3:** e02481.

Casadaban, M.J. (1976) Transposition and fusion of the *lac* genes to selected promoters in *Escherichia coli* using bacteriophage lambda and Mu. *J Mol Biol* **104:** 541–555.

Chaney, M., and Buck, M. (1999) The sigma 54 DNA-binding domain includes a determinant of enhancer responsiveness. *Mol Microbiol* **33:** 1200–1209.

Chaney, M., Grande, R., Wigneshweraraj, S.R., Cannon, W., Casaz, P., Gallegos, M.T., *et al*. (2001) Binding of transcriptional activators to σ^{54} in the presence of the transition state analog ADP-aluminum fluoride: insights into activator mechanochemical action. *Genes Dev* **15:** 2282–2294.

Chen, V.B., Arendall, W.B., 3rd, Headd, J.J., Keedy, D.A., Immormino, R.M., Kapral, G.J., *et al*. (2010) MolProbity: all-atom structure validation for macromolecular crystallography. *Acta Crystallogr D Biol Crystallogr* **66:** 12–21.

Copeland, R.A., Basavapathruni, A., Moyer, M., and Scott, M.P. (2011) Impact of enzyme concentration and residence time on apparent activity recovery in jump dilution analysis. *Anal Biochem* **416:** 206–210.

Darwin, A.J. (2005) The phage-shock-protein response. *Mol Microbiol* **57:** 621–628.

Datsenko, K.A., and Wanner, B.L. (2000) One-step inactivation of chromosomal genes in *Escherichia coli* K-12 using PCR products. *Proc Natl Acad Sci USA* **97:** 6640–6645.

De Carlo, S., Chen, B., Hoover, T.R., Kondrashkina, E., Nogales, E., and Nixon, B.T. (2006) The structural basis for regulated assembly and function of the transcriptional activator NtrC. *Genes Dev* **20:** 1485–1495.

Doucleff, M., Chen, B., Maris, A.E., Wemmer, D.E., Kondrashkina, E., and Nixon, B.T. (2005) Negative regulation of AAA + ATPase assembly by two component receiver domains: a transcription activation mechanism that is conserved in mesophilic and extremely hyperthermophilic bacteria. *J Mol Biol* **353:** 242–255.

Dworkin, J., Jovanovic, G., and Model, P. (2000) The PspA protein of *Escherichia coli* is a negative regulator of σ^{54}-dependent transcription. *J Bacteriol* **182:** 311–319.

Elderkin, S., Jones, S., Schumacher, J., Studholme, D., and Buck, M. (2002) Mechanism of action of the *Escherichia coli* phage shock protein PspA in repression of the AAA family transcription factor PspF. *J Mol Biol* **320:** 23–37.

Elderkin, S., Bordes, P., Jones, S., Rappas, M., and Buck, M. (2005) Molecular determinants for PspA-mediated repression of the AAA transcriptional activator PspF. *J Bacteriol* **187:** 3238–3248.

Emsley, P., Lohkamp, B., Scott, W.G., and Cowtan, K. (2010) Features and development of Coot. *Acta Crystallogr D Biol Crystallogr* **66:** 486–501.

Engl, C., Beek, A.T., Bekker, M., de Mattos, J.T., Jovanovic, G., and Buck, M. (2011) Dissipation of proton motive force is not sufficient to induce the phage shock protein response in *Escherichia coli*. *Curr Microbiol* **62:** 1374–1385.

Flores-Kim, J., and Darwin, A.J. (2015) Activity of a bacterial cell envelope stress response is controlled by the interaction of a protein binding domain with different partners. *J Biol Chem* **290:** 11417–11430.

Glynn, S.E., Martin, A., Nager, A.R., Baker, T.A., and Sauer, R.T. (2009) Structures of asymmetric ClpX hexamers reveal nucleotide-dependent motions in a AAA+ protein-unfolding machine. *Cell* **139:** 744–756.

Gruber, M., Soding, J., and Lupas, A.N. (2006) Comparative analysis of coiled-coil prediction methods. *J Struct Biol* **155:** 140–145.

Guex, N., and Peitsch, M.C. (1997) SWISS-MODEL and the Swiss-PdbViewer: an environment for comparative protein modeling. *Electrophoresis* **18:** 2714–2723.

Guzman, L.M., Belin, D., Carson, M.J., and Beckwith, J. (1995) Tight regulation, modulation, and high-level expression by vectors containing the arabinose P_{BAD} promoter. *J Bacteriol* **177:** 4121–4130.

Hankamer, B.D., Elderkin, S.L., Buck, M., and Nield, J. (2004) Organization of the AAA(+) adaptor protein PspA is an oligomeric ring. *J Biol Chem* **279:** 8862–8866.

Haslberger, T., Weibezahn, J., Zahn, R., Lee, S., Tsai, F.T., Bukau, B., and Mogk, A. (2007) M domains couple the ClpB threading motor with the DnaK chaperone activity. *Mol Cell* **25:** 247–260.

Hess, B., Kutzner, C., van der Spoel, D., and Lindahl, E. (2008) GROMACS 4: algorithms for highly efficient, load-balanced, and scalable molecular simulation. *J Chem Theory Comput* **4:** 435–447.

Holm, L., and Rosenstrom, P. (2010) Dali server: conservation mapping in 3D. *Nucleic Acids Res* **38:** W545–W549.

Holm, L., Kaariainen, S., Rosenstrom, P., and Schenkel, A. (2008) Searching protein structure databases with DaliLite v.3. *Bioinformatics* **24:** 2780–2781.

Horstman, N.K., and Darwin, A.J. (2012) Phage shock proteins B and C prevent lethal cytoplasmic membrane permeability in *Yersinia enterocolitica*. *Mol Microbiol* **85:** 445–460.

Joly, N., Schumacher, J., and Buck, M. (2006) Heterogeneous nucleotide occupancy stimulates functionality of phage shock protein F, an AAA+ transcriptional activator. *J Biol Chem* **281:** 34997–35007.

Joly, N., Burrows, P.C., Engl, C., Jovanovic, G., and Buck, M. (2009) A lower-order oligomer form of phage shock protein A (PspA) stably associates with the hexameric AAA(+) transcription activator protein PspF for negative regulation. *J Mol Biol* **394:** 764–775.

Joly, N., Engl, C., Jovanovic, G., Huvet, M., Toni, T., Sheng, X., *et al*. (2010) Managing membrane stress: the phage shock protein (Psp) response, from molecular mechanisms to physiology. *FEMS Microbiol Rev* **34:** 797–827.

Jordan, S., Junker, A., Helmann, J.D., and Mascher, T. (2006) Regulation of LiaRS-dependent gene expression in *Bacillus subtilis*: identification of inhibitor proteins, regulator binding sites, and target genes of a conserved cell envelope stress-sensing two-component system. *J Bacteriol* **188:** 5153–5166.

Jovanovic, G., Weiner, L., and Model, P. (1996) Identification, nucleotide sequence, and characterization of PspF, the transcriptional activator of the *Escherichia coli* stress-induced psp operon. *J Bacteriol* **178:** 1936–1945.

Jovanovic, G., Dworkin, J., and Model, P. (1997) Autogenous control of PspF, a constitutively active enhancer-binding protein of *Escherichia coli*. *J Bacteriol* **179:** 5232–5237.

Jovanovic, G., Mehta, P., McDonald, C., Davidson, A.C., Uzdavinys, P., Ying, L., and Buck, M. (2014) The N-terminal amphipathic helices determine regulatory and effector functions of phage shock protein A (PspA) in *Escherichia coli*. *J Mol Biol* **426:** 1498–1511.

Kabsch, W. (2010) Xds. *Acta Crystallogr D Biol Crystallogr* **66:** 125–132.

Kammerer, R.A., Kostrewa, D., Progias, P., Honnappa, S., Avila, D., Lustig, A., *et al*. (2005) A conserved trimerization motif controls the topology of short coiled coils. *Proc Natl Acad Sci USA* **102:** 13891–13896.

Kroll, D., Meierhoff, K., Bechtold, N., Kinoshita, M., Westphal, S., Vothknecht, U.C., *et al*. (2001) *VIPP1*, a nuclear gene of *Arabidopsis thaliana* essential for thylakoid membrane formation. *Proc Natl Acad Sci USA* **98:** 4238–4242.

Langer, G., Cohen, S.X., Lamzin, V.S., and Perrakis, A. (2008) Automated macromolecular model building for X-ray crystallography using ARP/wARP version 7. *Nat Protoc* **3:** 1171–1179.

Lanzetta, P.A., Alvarez, L.J., Reinach, P.S., and Candia, O.A. (1979) An improved assay for nanomole amounts of inorganic phosphate. *Anal Biochem* **100:** 95–97.

Lee, H., Park, H., Ko, J., and Seok, C. (2013) GalaxyGemini: a web server for protein homo-oligomer structure prediction based on similarity. *Bioinformatics* **29:** 1078–1080.

Lee, S., Sowa, M.E., Watanabe, Y.H., Sigler, P.B., Chiu, W., Yoshida, M., and Tsai, F.T. (2003) The structure of ClpB: a molecular chaperone that rescues proteins from an aggregated state. *Cell* **115:** 229–240.

Lenn, T., Gkekas, C.N., Bernard, L., Engl, C., Jovanovic, G., Buck, M., and Ying, L. (2011) Measuring the stoichiometry of functional PspA complexes in living bacterial cells by single molecule photobleaching. *Chem Commun (Camb)* **47:** 400–402.

Li, G.W., Burkhardt, D., Gross, C., and Weissman, J.S. (2014) Quantifying absolute protein synthesis rates reveals principles underlying allocation of cellular resources. *Cell* **157:** 624–635.

Lindenstrauss, U., Matos, C.F., Graubner, W., Robinson, C., and Bruser, T. (2010) Malfolded recombinant Tat substrates are Tat-independently degraded in *Escherichia coli*. *FEBS Lett* **584:** 3644–3648.

Lindorff-Larsen, K., Piana, S., Palmo, K., Maragakis, P.,

Klepeis, J.L., Dror, R.O., and Shaw, D.E. (2010) Improved side-chain torsion potentials for the Amber ff99SB protein force field. *Proteins* **78:** 1950–1958.
Lum, R., Tkach, J.M., Vierling, E., and Glover, J.R. (2004) Evidence for an unfolding/threading mechanism for protein disaggregation by *Saccharomyces cerevisiae* Hsp104. *J Biol Chem* **279:** 29139–29146.
Lupas, A., Van Dyke, M., and Stock, J. (1991) Predicting coiled coils from protein sequences. *Science* **252:** 1162–1164.
Mehta, P., Jovanovic, G., Lenn, T., Bruckbauer, A., Engl, C., Ying, L., and Buck, M. (2013) Dynamics and stoichiometry of a regulated enhancer-binding protein in live *Escherichia coli* cells. *Nat Commun* **4:** 1997.
Miller, J.H. (1972) *Experiments in molecular genetics*, p. XVI, 466 S. Cold Spring Harbor Laboratory, Cold Spring Harbor.
Model, P., Jovanovic, G., and Dworkin, J. (1997) The *Escherichia coli* phage-shock-protein (*psp*) operon. *Mol Microbiol* **24:** 255–261.
Mogk, A., Schlieker, C., Strub, C., Rist, W., Weibezahn, J., and Bukau, B. (2003) Roles of individual domains and conserved motifs of the AAA+ chaperone ClpB in oligomerization, ATP hydrolysis, and chaperone activity. *J Biol Chem* **278:** 17615–17624.
Murshudov, G.N., Vagin, A.A., and Dodson, E.J. (1997) Refinement of macromolecular structures by the maximum-likelihood method. *Acta Crystallogr D Biol Crystallogr* **53:** 240–255.
Neuwald, A.F., Aravind, L., Spouge, J.L., and Koonin, E.V. (1999) AAA+: a class of chaperone-like ATPases associated with the assembly, operation, and disassembly of protein complexes. *Genome Res* **9:** 27–43.
Oguchi, Y., Kummer, E., Seyffer, F., Berynskyy, M., Anstett, B., Zahn, R., *et al*. (2012) A tightly regulated molecular toggle controls AAA+ disaggregase. *Nat Struct Mol Biol* **19:** 1338–1346.
Overmann, J., Fischer, U., and Pfennig, N. (1992) A new purple sulfur bacterium from saline littoral sediments, *Thiorhodovibrio winogradskyi* Gen-Nov and Sp-Nov. *Arch Microbiol* **157:** 329–335.
Possot, O., d'Enfert, C., Reyss, I., and Pugsley, A.P. (1992) Pullulanase secretion in *Escherichia coli* K-12 requires a cytoplasmic protein and a putative polytopic cytoplasmic membrane protein. *Mol Microbiol* **6:** 95–105.
Punta, M., Coggill, P.C., Eberhardt, R.Y., Mistry, J., Tate, J., Boursnell, C., *et al*. (2012) The Pfam protein families database. *Nucleic Acids Res* **40:** D290–D301.
Rappas, M., Schumacher, J., Beuron, F., Niwa, H., Bordes, P., Wigneshweraraj, S., *et al*. (2005) Structural insights into the activity of enhancer-binding proteins. *Science* **307:** 1972–1975.
Rappas, M., Schumacher, J., Niwa, H., Buck, M., and Zhang, X. (2006) Structural basis of the nucleotide driven conformational changes in the AAA+ domain of transcription activator PspF. *J Mol Biol* **357:** 481–492.
Sambrook, J., and Russell, D.W. (2001) *Molecular Cloning a Laboratory Manual*. Cold Spring Harbor, NY: Cold Spring Harbor Laboratory Press.
Schirmer, E.C., Homann, O.R., Kowal, A.S., and Lindquist, S. (2004) Dominant gain-of-function mutations in Hsp104p reveal crucial roles for the middle region. *Mol Biol Cell* **15:** 2061–2072.
Schrodinger, L.L.C. (2010) The PyMOL Molecular Graphics System, Version 1.3r1.
Schuck, P. (2000) Size-distribution analysis of macromolecules by sedimentation velocity ultracentrifugation and lamm equation modeling. *Biophys J* **78:** 1606–1619.
Schumacher, J., Zhang, X., Jones, S., Bordes, P., and Buck, M. (2004) ATP-dependent transcriptional activation by bacterial PspF AAA+protein. *J Mol Biol* **338:** 863–875.
Seyffer, F., Kummer, E., Oguchi, Y., Winkler, J., Kumar, M., Zahn, R., *et al*. (2012) Hsp70 proteins bind Hsp100 regulatory M domains to activate AAA+ disaggregase at aggregate surfaces. *Nat Struct Mol Biol* **19:** 1347–1355.
Sharma, A., Leach, R.N., Gell, C., Zhang, N., Burrows, P.C., Shepherd, D.A., *et al*. (2014) Domain movements of the enhancer-dependent sigma factor drive DNA delivery into the RNA polymerase active site: insights from single molecule studies. *Nucleic Acids Res* **42:** 5177–5190.
Sheldrick, G.M. (2010) Experimental phasing with SHELXC/D/E: combining chain tracing with density modification. *Acta Crystallogr D Biol Crystallogr* **66:** 479–485.
Standar, K., Mehner, D., Osadnik, H., Berthelmann, F., Hause, G., Lunsdorf, H., and Bruser, T. (2008) PspA can form large scaffolds in *Escherichia coli*. *FEBS Lett* **582:** 3585–3589.
Syed, A., and Gralla, J.D. (1997) Isolation and properties of enhancer-bypass mutants of sigma 54. *Mol Microbiol* **23:** 987–995.
Sysoeva, T.A., Chowdhury, S., Guo, L., and Nixon, B.T. (2013) Nucleotide-induced asymmetry within ATPase activator ring drives σ^{54}-RNAP interaction and ATP hydrolysis. *Genes Dev* **27:** 2500–2511.
Thomason, L.C., Costantino, N., and Court, D.L. (2007) *E. coli* genome manipulation by P1 transduction. Curr Protoc Mol Biol Chapter 1: Unit 1 17.
Tummino, P.J., and Copeland, R.A. (2008) Residence time of receptor-ligand complexes and its effect on biological function. *Biochemistry* **47:** 5481–5492.
Turgay, K., Hamoen, L.W., Venema, G., and Dubnau, D. (1997) Biochemical characterization of a molecular switch involving the heat shock protein ClpC, which controls the activity of ComK, the competence transcription factor of *Bacillus subtilis*. *Genes Dev* **11:** 119–128.
Valgepea, K., Adamberg, K., Seiman, A., and Vilu, R. (2013) *Escherichia coli* achieves faster growth by increasing catalytic and translation rates of proteins. *Mol Biosyst* **9:** 2344–2358.
Van Duyne, G.D., Standaert, R.F., Karplus, P.A., Schreiber, S.L., and Clardy, J. (1993) Atomic structures of the human immunophilin FKBP-12 complexes with FK506 and rapamycin. *J Mol Biol* **229:** 105–124.
Vonrhein, C., Blanc, E., Roversi, P., and Bricogne, G. (2007) Automated structure solution with autoSHARP. *Methods Mol Biol* **364:** 215–230.
Waterhouse, A.M., Procter, J.B., Martin, D.M., Clamp, M., and Barton, G.J. (2009) Jalview version 2 – a multiple sequence alignment editor and analysis workbench. *Bioinformatics* **25:** 1189–1191.
Weber, A., Kogl, S.A., and Jung, K. (2006) Time-dependent proteome alterations under osmotic stress during aerobic

and anaerobic growth in *Escherichia coli*. *J Bacteriol* **188:** 7165–7175.
Wilms, B., Hauck, A., Reuss, M., Syldatk, C., Mattes, R., Siemann, M., and Altenbuchner, J. (2001) High-cell-density fermentation for production of L-*N*-carbamoylase using an expression system based on the *Escherichia coli rhaBAD* promoter. *Biotechnol Bioeng* **73:** 95–103.
Winn, M.D., Ballard, C.C., Cowtan, K.D., Dodson, E.J., Emsley, P., Evans, P.R., *et al*. (2011) Overview of the CCP4 suite and current developments. *Acta Crystallogr D Biol Crystallogr* **67:** 235–242.
Woo, K.M., Kim, K.I., Goldberg, A.L., Ha, D.B., and Chung, C.H. (1992) The heat-shock protein ClpB in *Escherichia coli* is a protein-activated ATPase. *J Biol Chem* **267:** 20429–20434.
Yamaguchi, S., and Darwin, A.J. (2012) Recent findings about the *Yersinia enterocolitica* phage shock protein response. *J Microbiol* **50:** 1–7.
Yamaguchi, S., Gueguen, E., Horstman, N.K., and Darwin, A.J. (2010) Membrane association of PspA depends on activation of the phage-shock-protein response in *Yersinia enterocolitica*. *Mol Microbiol* **78:** 429–443.
Yamaguchi, S., Reid, D.A., Rothenberg, E., and Darwin, A.J. (2013) Changes in Psp protein binding partners, localization and behaviour upon activation of the *Yersinia enterocolitica* phage shock protein response. *Mol Microbiol* **87:** 656–671.
Zhang, N., Simpson, T., Lawton, E., Uzdavinys, P., Joly, N., Burrows, P., and Buck, M. (2013) A key hydrophobic patch identified in an AAA(+) protein essential for its in trans inhibitory regulation. *J Mol Biol* **425:** 2656–2669.

Supporting information

Additional supporting information may be found in the online version of this article at the publisher's web-site.